FULL-SCALE EARTHQUAKE EXPERIMENT OF ELECTRIC EQUIPMENT

W. M. Dong (I)
S. R. Zhou (II)
Presenting Author: W. M. Dong

SUMMARY

Many types of electric equipment are vulnerable to earthquake ground motion. In order to investigate their seismic behavior, full-scale tests of circuit breakers and lightning arresters were conducted. For improving the performance of the equipment, steel-laminated rubber cushions were used to isolate the equipment from the input motions.

In this paper, the results of these experiments are compared with the analytical investigations, using a linear model. The agreement between the analytical and the experimental results is good. The experiments indicate that the well-designed base isolator can substantially reduce the earthquake response, and in some cases, the reduction can be 30-50%.

INTRODUCTION

Many substations have suffered serious damage in recent earthquakes. Some electric equipment, such as circuit breakers, are made of brittle material and have shown very poor performance in past earthquakes (Fig. 1). According to the tests conducted on site and in the laboratory, the natural frequency of these breakers are in the range of 2.2-4.4 HZ, which approximates the predominant frequency of the earthquake ground motion. In addition, the small damping of this equipment builds up the response significantly during an earthquake. The dynamic analysis conducted for 220 KV circuit breaker indicates that the response bending moment at the bottom due to the 1940 El Centro earthquake and the 1976 Ninghe earthquake (0.4g) are 1.68 and 1.85 (T-M), respectively, which are greater than the average static ultimate capacity 1.39 (T-M) (Ref. 1). This implies that most of these breakers would be damaged in the El Centro type earthquake or other earthquakes with intensity IX. The major cause for the damage is the pseudo resonance induced by the earthquake. In order to improve the performance of these equipments, steel-laminated rubber cushions have been suggested to isolate the ground motion (Ref. 2). The purpose of the experiment was intended to varify the validation of the isolator.

DESIGNS OF THE ISOLATORS

The steel-laminated rubber is used as an isolator (Fig. 2). Under the shear and axial force, the deformation of rubber layer is shown in Fig. 3, and the horizontal and vertical stiffnesses, k_H and k_V, are

(I) Engineer, XINGHUA Engineering Consulting Corp., Beijing, China
(II) Engineer, XINGHUA Engineering Consulting Corp., Beijing, China

respectively:

$$k_H = \xi G \quad (\pi R^2 / h) \qquad (1)$$

$$k_V = \Phi \xi \quad E(\pi R^2 / h) \qquad (2)$$

where G and E - static shear and compressive modulus of rubber (in kg/cm^2)
R - radius of rubber layer;
h - thickness of rubber layer;
ξ - ratio between dynamic and static stiffness;
ϕ - shape factor, which is estimated by

$$\phi \cong 1.2 \left[1+1.65(R/2h)^2 \right]$$

Let n be the number of rubber layers, then the dynamic horizontal and vertical stiffnesses, K_H and K_V, are respectively:

$$K_H = k_H / n \qquad (3)$$

$$K_V = k_V / n \qquad (4)$$

The isolators installed under the breaker can be modeled as a shear spring and a rotation spring (Fig. 4) with their stiffnesses K_B and K_θ as

$$K_B = m \times K_H \qquad (5)$$

$$K_\theta = m \times K_V \times \ell^2 \qquad (6)$$

where m - number of isolators;
ℓ - distance from the isolator to the center of the breaker.

Two types of isolators, A and B, were used in the experiment. Their parameters are:

$G = 6.8 kg/cm^2$, $E = 19 kg/cm^2$, $\xi = 1.2$,

$R = 4$ cm, $h = 1.2$ cm, $\ell = 40$ cm.

Hence, for Type A (n=12), the shear and rotation stiffnesses are, respectively,

$K_B = 114$ kg/cm, $K_\theta = 4.84 \times 10^6$ kg-cm/rad.

for type B (n=9), $K_B = 152$ kg/cm, $K_\theta = 6.45 \times 10^6$ kg-cm/rad.

DYNAMIC MODEL

The breaker and isolator are modeled as a system of multi-degrees of freedom (Fig. 5). Under the excitation of ground motion $\ddot{x}_g$, the equation of motion of the system is:

$$[M] \{ \ddot{Y} \} + [C] \{ Y \} + [K] \{ Y \} = - \{ M_o \} \ddot{x}_g \qquad (7)$$

where

$$[M] = \begin{bmatrix} m_B & & & & 0 \\ & m_1 & & & \\ & & m_2 & & \\ & & & \ddots & \\ 0 & & & & m_N \\ & & & & & I \end{bmatrix}$$

$$\{ M_o \} = \{ m_B, m_1, m_2, \ldots\ldots m_n, 0 \}^T$$

$$\{ Y \} = \{ y_b, y_1, y_2, \ldots\ldots y_n, \theta \}^T$$

$$[K] = \begin{bmatrix} K_B + \{1\}^T [K]_r \{1\} & -\{1\}^T [K]_r & \{1\}^T [K]_r \{H\} \\ -[K]_r \{1\} & [K]_r & -[K]_r \{H\} \\ \{H\}^T [K] \{1\} & \{H\}^T [K]_r & K_\theta + \{H\}^T [K]_r \{H\} \end{bmatrix}$$

$$[K]_r = \begin{bmatrix} k_{11} & k_{12} & \ldots\ldots & k_{1n} \\ & k_{22} & \ldots\ldots & k_{2n} \\ \text{syn.} & & & k_{nn} \end{bmatrix}$$

$$\{ H \} = \{ k_1, k_2, \ldots\ldots k_n \}^T$$

$$\{ 1 \} = \{ 1, 1, \ldots\ldots 1 \}^T$$

$$[C] = \alpha [M] + \beta [K]$$

m_B = mass of the rack

I = moment of inertia of the rack

α and β - coefficients

The dynamic response of the system is obtained by the linear acceleration method.

SHAKING TABLE TESTS

The 220 KV and 110 KV breakers (SW-220 and SW-110) were tested with and without isolators. Fig. 6 shows the breaker mounted on the table. Fig. 7 indicates the arrangement of the instruments. Some results of the test are as follows:

1, The stiffnesses and damping of the isolators (type-A and type-B)

were measured, and showed good agreement with the estimated values in design (Table 1).

2, The natural frequencies and dampings of the breakers with and without isolators were measured. The results are shown in Table 2, in which the computed values, based on the model of multi-degrees of freedom, are also listed. The natural frequencies for the circuit breaker with isolators are reduced to 53% (for SW-220) and 38% (for SW-110) of those without isolators. The damping is increased by more than 2 times.

3, Sine wave sweep tests and destruction tests were conducted on the shaking table. Fig. 8 gives the responses of the breakers SW-110 and SW-110 under 0.025,0.05,0.1g input levels. With the increase of the input level, the resonant frequency shifted to the lower value, indicating a slight non-linearity. Fig. 9 shows the comparision of the acceleration responses between SW-220 and SW_B-220. Due to the installation of isolators, the acceleration response was reduced to less than 0.5 times.

The first two modes of SW-110 obtained in the resonant frequencies are shown in Fig. 10, where the numbers in parentheses were calculated from the model. The agreement is good. Note that the breaker moves on the isolators like a rigid body, the deformation of breaker itself is negligible.

4, The strain responses at the bottom of breaker to the El Centro earthquake were recorded (Fig. 11). The time histories show apparently the filtering effects of the system. The dominant frequencies are 2.3 HZ and 1.2 HZ for SW-220 and SW_B-220. The response of the circuit breaker with isolators was significantly reduced, but the displacement was increased. Table 3 gives the comparison of the responses between the breakers with and without isolators.

5, Destructive tests were conducted on the shaking table. The stresses and the bending moments at failure of the breaker are given in Table 4, where the only data obtained were from the breakers without isolators. Those breakers with isolators could not be destroyed until the input acceleration reached the limit of the table (0.4g). Fig. 12 shows the broken equipment.

6, The lightning arresters were tested for their dynamic characteristics. The natural frequency is about 4 (HZ) and the damping is around 2%. The ultimate stress at rupture is near the one for the breakers.

CONCLUSION

Based upon the experimental investigations, the following conclusions can be reached:

1, The damage to the circuit breaker was caused by its pseudo resonance during the earthquake, resulting in sudden rupture of the brittle porcelain column.

2, The ultimate stress of the available porcelain column is in the range of 140-180 kg/cm^2, which can be referred to in aseismic design.

3, The laminated cushion can isolate the groud motion effectively, resulting in the stress reduction of 34-53% of the original.

4, The model of multi-degrees of freedom system can be used to evaluate the frequency and the dynamic response of the system with reasonable accuracy.

5, In order to reduce the rotation of the breaker on the isolators, it is suggested that the vertical stiffness should be increased under the condition that the shear stiffness in not increased. It can be achieved by decreasing the thickness of rubber layer.

6, In the area where local soil is soft, it is not recommended to use such an isolation system.

ACKNOWLEDGEMENT

The authors gratefully acknowledge the South-West Building Research Institute and the Harbin Engineering Mechanics Institute for providing the experiment facilities and technical help.

REFERENCES

(1) Tung (Dong), W. and S. Zhou, "An Investigation of Earthquake Damage to Electrical Equipment", ASME, Century 2 Pressure Vessels and Piping Conference, San Francisco 1980. Paper 80 - C2/PVP-85.

(2) Kircher, C. A. et al, "Performance of A 230 KV ATB 7 Power Circuit Breaker Mounted on GAPEC Seismic Isolators" Report No. 40, 1979. The John A. Blume Earthquake Engineering Center, Stanford University.

Table 1

Type of isolator	shear stiff. K_B(kg/cm)		rotation stiff. K_0(kg-cm/rad.)		damping (%)
	measured	estimated	measured	estimated	
A	112	114	$4.8*10^6$	$4.84*10^6$	6-7
B	144	152	$6.72*10^6$	$6.54*10^6$	

Table 2

Type of sample	Natural frequency(hz)		measured damping (%)
	measured	calculated	
SW-110	4.08-4.4	4.01	2.3
SW_A-110	1.45	1.43	10.0
SW_B-110	1.60	1.63	5.3-5.9
SW-220	2.16-2.54	2.16	2.0-3.3
SW_B-220	1.23	1.19	4.93

Table 3

Type of samples	Peak acce. imputed (g)	The measured		That scaled to 0.34g acce.	
		acce. at top A (g)	stress at bottom σ(kg/cm^2)	A	σ
SW-220	0.34	1.31	161	1.31	161
SW_B-220	0.42	0.56	68.5	0.45	55.4
The reduction effectiveness				65.7%	65.6%
SW-110	0.61	1.35	146.8	0.75	81.8
SW_B-110	0.645	0.74	83.0	0.39	43.8
The reduction effectiveness				48.0%	46.5%

Table 4

No. of samples	Type of input	Section Size	The ultimate stress (kg/cm^2)	The ultimate moment (T-M)
SW-1	sinosoidal	The outer	164.8	1.76
SW-3	sinosoidal	diameter	141.0	1.51
SW-5		D=2.5cm	142.3	1.52
SW-4	El center	The inner	161.0	1.72
SW-6	El center	diameter d=18.5cm	181.0	1.94

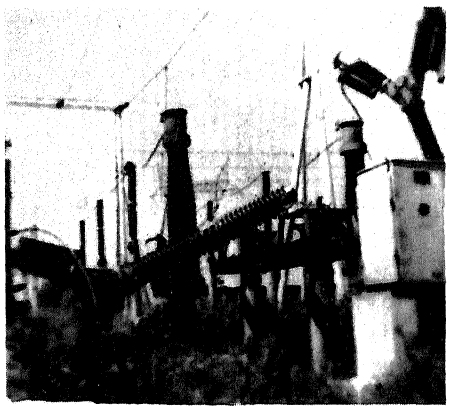

Fig. 1

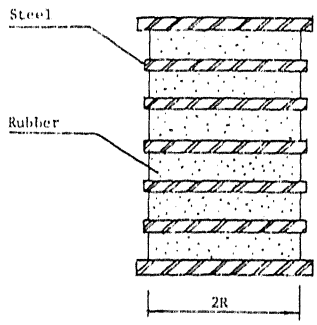

Fig. 2

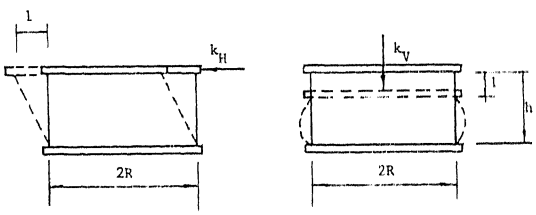

Fig. 3

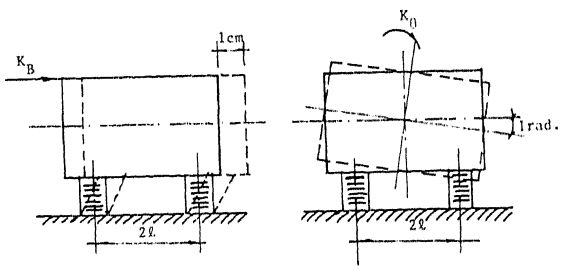

Fig. 4

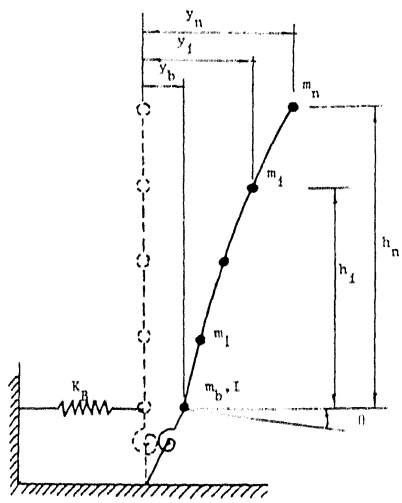

Fig. 5

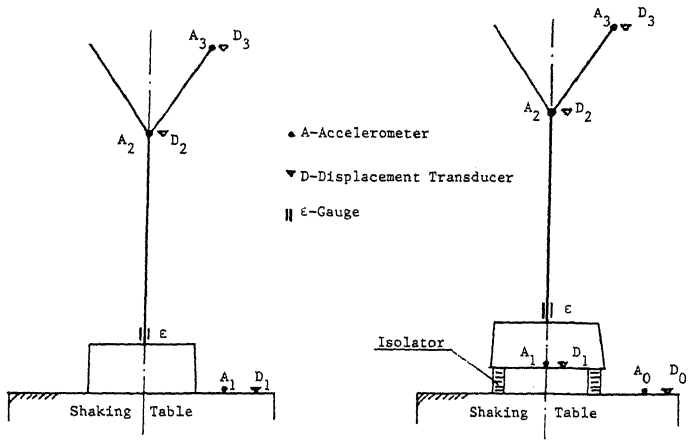
A3
D3
A2
D2
A-Accelerometer
D-Displacement Transducer
ε-Gauge
ε
A1
D1
Shaking Table
Isolator
A0
D0

Fig. 7

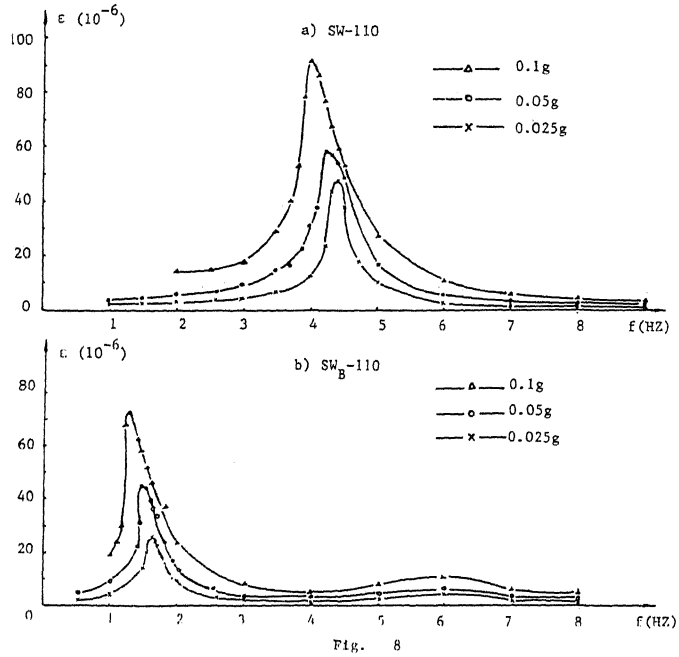
ε (10⁻⁶)
a) SW-110
0.1g
0.05g
0.025g
f(HZ)
b) SW_B-110

Fig. 8

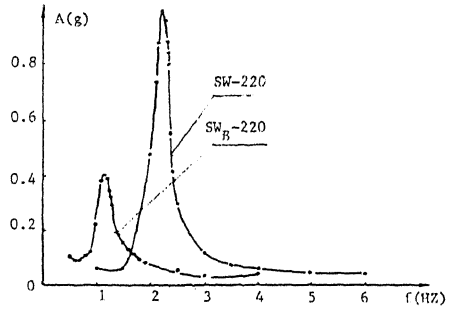

Fig. 9

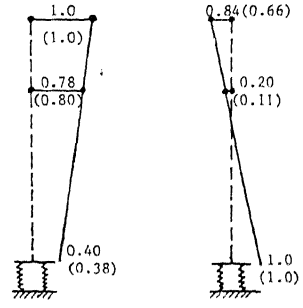

f_1=1.45(1.43)HZ f_2=4.17(4.46)HZ

Fig. 10

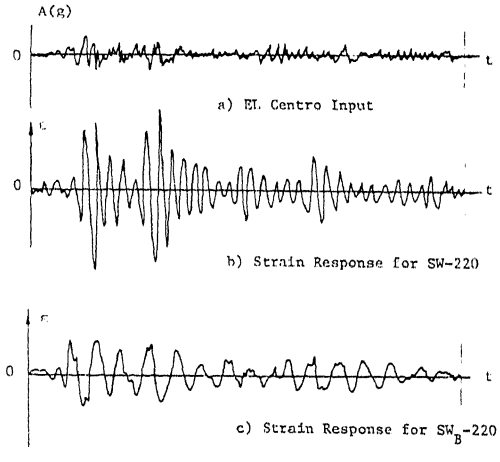

Fig. 11

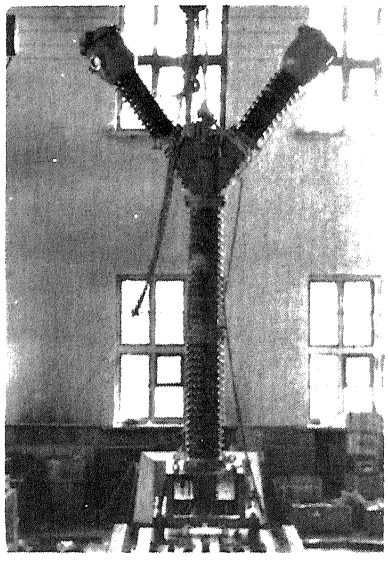

Fig. 6

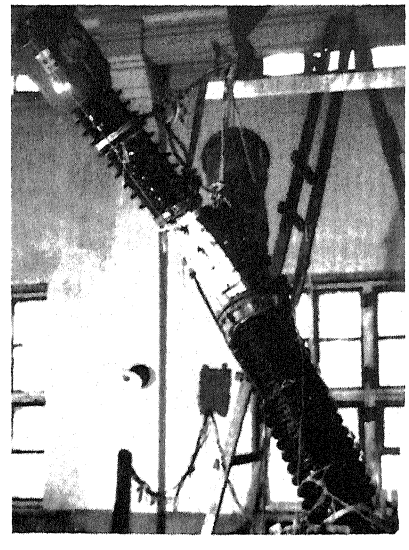

Fig. 12